

X-ray third-order nonlinear plane-wave Bragg-case dynamical diffraction effects in a perfect crystal. Erratum

Minas K. Balyan*

Faculty of Physics, Department of Solid State Physics, Yerevan State University, Alex Manoogian 1, Yerevan 0025, Armenia. *Correspondence e-mail: mbalyan@ysu.am

Received 11 June 2016
Accepted 15 June 2016

Edited by A. Momose, Tohoku University, Japan

Keywords: nonlinear diffraction; Bragg case; reflection region; third-order nonlinearity; two-wave diffraction

Formulae in the paper by Balyan (2015) [*J. Synchrotron Rad.* **22**, 1410–1418] are corrected.

The formulae (2) and (4) in the paper Balyan (2015) have the same essential typographical error. The correct forms of these equations are

$$\text{rot rot } \tilde{\mathbf{E}} + \frac{1}{c^2} \frac{\partial^2 \tilde{\mathbf{E}}}{\partial t^2} = -\frac{1}{\epsilon_0 c^2} \frac{\partial^2 \tilde{\mathbf{P}}}{\partial t^2} \quad (2)$$

and

$$\text{rot rot } \tilde{\mathbf{E}}(\mathbf{r}, \omega_q) - \frac{\omega_q^2}{c^2} [1 + \chi^{(1)}(\mathbf{r}, \omega_q)] \tilde{\mathbf{E}}(\mathbf{r}, \omega_q) = \frac{\omega_q^2}{\epsilon_0 c^2} \tilde{\mathbf{P}}^{\text{NL}}(\mathbf{r}, \omega_q). \quad (4)$$

In the same paper, the formulae (17) and (19) are also incorrect. The correct forms of these equations are

$$E^{(i)}(x, 0) = E_0^{(i)} \exp(ik \cos \theta^{(i)} x) \quad (17)$$

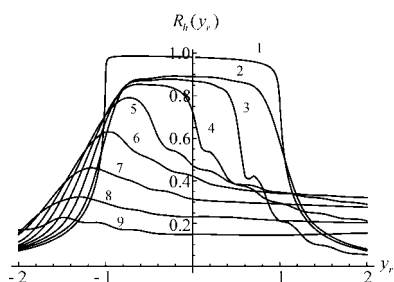
and

$$\begin{aligned} E_0(x, 0) &= E_0^{(i)} \exp(-ik \sin \theta \Delta \theta x), \\ E_h(x, T) &= 0. \end{aligned} \quad (19)$$

These equations are used for derivation of the third-order nonlinear Takagi's equations.

References

Balyan, M. K. (2015). *J. Synchrotron Rad.* **22**, 1410–1418.



X-ray third-order nonlinear plane-wave Bragg-case dynamical diffraction effects in a perfect crystal

Minas K. Balyan*

Faculty of Physics, Department of Solid State Physics, Yerevan State University, Alex Manoogian 1, Yerevan 0025, Armenia. *Correspondence e-mail: mbalyan@ysu.am

Received 6 April 2015

Accepted 22 September 2015

Edited by A. Momose, Tohoku University, Japan

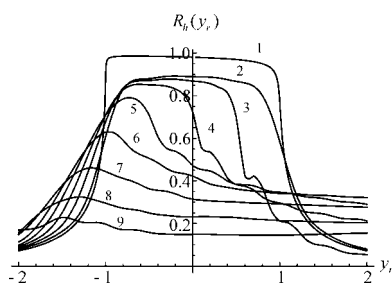
Keywords: nonlinear diffraction; Bragg case; reflection region; third-order nonlinearity; two-wave diffraction.

Two-wave symmetric Bragg-case dynamical diffraction of a plane X-ray wave in a crystal with third-order nonlinear response to the electric field is considered theoretically. For certain diffraction conditions for a non-absorbing perfect semi-infinite crystal in the total reflection region an analytical solution is found. For the width and for the center of the total reflection region expressions on the intensity of the incidence wave are established. It is shown that in the nonlinear case the total reflection region exists below a maximal intensity of the incidence wave. With increasing intensity of the incidence wave the total reflection region's center moves to low angles and the width decreases. Using numerical calculations for an absorbing semi-infinite crystal, the behavior of the reflected wave as a function of the intensity of the incidence wave and of the deviation parameter from the Bragg condition is analyzed. The results of numerical calculations are compared with the obtained analytical solution.

1. Introduction

The success of high-intensity X-ray synchrotron sources and X-ray free-electron lasers (XFELs) has brought about theoretical and experimental investigations of nonlinear X-ray diffraction and other nonlinear effects of X-ray interaction with matter. X-ray dynamical diffraction is described by Takagi's equations (Takagi, 1969). Starting from the wave equation for a monochromatic component and replacing the linear susceptibility by a third-order nonlinear one, nonlinear Takagi's equations can also be obtained. Nazarkin *et al.* (2003), using the cold collisionless plasma model, studied the linear dynamical diffraction of the X-ray second-order harmonic formed in a perfect crystal under two-wave diffraction conditions. The backward influence of two Bragg-diffracted waves on the amplitude of the incidence wave was not considered. Tamasaku & Ishikawa (2007*a,b*), not using the cold plasma model, investigated the kinematical diffraction of an X-ray plane wave under second-order nonlinearity conditions with parametric down-conversion of an X-ray photon into an X-ray low-frequency photon and a UV photon. Conti *et al.* (2008), using the third-order nonlinear cold plasma model, investigated the direct propagation of an intense X-ray beam. Other nonlinear X-ray effects (two-photon absorption and so on) have been investigated as well (Tamasaku *et al.*, 2014; Doumi *et al.*, 2011; Son *et al.*, 2011, and references therein).

For low-intensity X-ray incidence waves the electrons of matter oscillate as linear oscillators; meanwhile, increasing



intensity enforces electrons to oscillate as nonlinear oscillators. Thus, the nonlinear model of visible light optics can be used for X-rays until the perturbation theory is valid. It should also be mentioned that nonlinear effects can also be observed for low-intensity waves, since the accumulation effect of nonlinear polarization influences the propagation of the wave a sufficient distance in a nonlinear media. In Balyan (2015) the third-order nonlinear Takagi's equations are obtained.

In this paper, third-order nonlinear Takagi's equations are written using the model of visible light optics, considering a crystal as an isotropic media, as in the linear theory of diffraction. Based on nonlinear Takagi's equations, symmetric Bragg-case third-order nonlinear dynamical diffraction of a plane σ -polarized monochromatic wave in a perfect crystal is investigated theoretically. In the total reflection region an analytical solution is obtained in a non-absorbing semi-infinite crystal. The dependence of the center and of the width of the total reflection region on the intensity of the incidence wave is found. The results of numerical calculations of rocking curves, provided for an absorbing crystal, are compared with the findings of analytical solutions.

2. Third-order nonlinear Takagi's equations

X-rays are mainly scattered by the bound electrons of each atom in nonlinear media (James, 1950). The scattering on valence electrons is small. The nonlinearity of the motion of each bound electron may be considered both classically and quantum-mechanically. The restoring force in the nonlinear case has a nonlinear component (Boyd, 2003). The frequency of the incidence radiation is larger than the maximal resonance frequency of electrons. In a nonlinear non-magnetic medium the electrical field and polarization have the forms

$$\begin{aligned}\tilde{\mathbf{E}}(\mathbf{r}, t) &= \sum_q \tilde{\mathbf{E}}(\mathbf{r}, \omega_q) \exp(-i\omega_q t), \\ \tilde{\mathbf{P}}(\mathbf{r}, t) &= \sum_q \tilde{\mathbf{P}}(\mathbf{r}, \omega_q) \exp(-i\omega_q t).\end{aligned}\quad (1)$$

Here ω_q are all possible frequencies (negative and positive) in the nonlinear case. Since $\tilde{\mathbf{E}}$ and $\tilde{\mathbf{P}}$ are real, then $\tilde{\mathbf{E}}(\mathbf{r}, \omega_q) = \tilde{\mathbf{E}}^*(\mathbf{r}, -\omega_q)$ and $\tilde{\mathbf{P}}(\mathbf{r}, \omega_q) = \tilde{\mathbf{P}}^*(\mathbf{r}, -\omega_q)$. The wave equation for electrical field strength is (Boyd, 2003)

$$\tilde{\mathbf{E}} + \frac{1}{c^2} \frac{\partial^2 \tilde{\mathbf{E}}}{\partial t^2} = -\frac{1}{\varepsilon_0 c^2} \frac{\partial^2 \tilde{\mathbf{P}}}{\partial t^2}.\quad (2)$$

Here c is the velocity of light in free space and $\varepsilon_0 = 8.85 \times 10^{-12} \text{ F m}^{-1}$ is the permittivity of free space. It is convenient to present the polarization as the sum of linear and nonlinear components,

$$\tilde{\mathbf{P}}(\mathbf{r}, \omega_q) = \tilde{\mathbf{P}}^{(1)}(\mathbf{r}, \omega_q) + \tilde{\mathbf{P}}^{\text{NL}}(\mathbf{r}, \omega_q).\quad (3)$$

Here $\tilde{\mathbf{P}}^{(1)}(\mathbf{r}, \omega_q) = \varepsilon_0 \chi^{(1)}(\mathbf{r}, \omega_q) \tilde{\mathbf{E}}(\mathbf{r}, \omega_q)$ is the part of the polarization depending linearly on the strength of the electrical field. The crystal, as in the linear theory, may be considered as isotropic media and susceptibility $\chi^{(1)}(\mathbf{r}, \omega_q)$ is a

scalar. $\tilde{\mathbf{P}}^{\text{NL}}(\mathbf{r}, \omega_q)$ is the nonlinear part of the polarization. Inserting (1) and (3) into (2), one finds the wave equation for each frequency,

$$\tilde{\mathbf{E}}(\mathbf{r}, \omega_q) - \frac{\omega_q^2}{c^2} [1 + \chi^{(1)}(\mathbf{r}, \omega_q)] \tilde{\mathbf{E}}(\mathbf{r}, \omega_q) = \frac{\omega_q^2}{\varepsilon_0 c^2} \tilde{\mathbf{P}}^{\text{NL}}(\mathbf{r}, \omega_q).\quad (4)$$

The third-order susceptibility fourth-rank tensor $\chi_{ijkl}^{(3)}(\omega_q; \omega_m, \omega_n, \omega_p, \mathbf{r})$ is introduced according to the relation (Boyd, 2003)

$$\begin{aligned}\tilde{\mathbf{P}}_i^{(3)}(\mathbf{r}, \omega_q) &= \varepsilon_0 \sum_{(mnp)} \chi_{ijkl}^{(3)}(\omega_q; \omega_m, \omega_n, \omega_p, \mathbf{r}) \\ &\times \tilde{E}_j(\mathbf{r}, \omega_m) \tilde{E}_k(\mathbf{r}, \omega_n) \tilde{E}_l(\mathbf{r}, \omega_p),\end{aligned}\quad (5)$$

where the summation is performed over all frequencies $\omega_m, \omega_n, \omega_p$ so that $\omega_q = \omega_m + \omega_n + \omega_p$ and over all dummy indices $j, k, l = 1, 2, 3$ corresponding to Cartesian coordinates x, y, z . Each term on the right-hand side of (5) corresponds to a frequency mixing nonlinear process if at least two frequencies are different. If all three frequencies are the same and one of them is negative, the corresponding ω_q is the same. Such terms in (5) describe the propagation of the wave in a nonlinear media with self-induced refractive index. In a perfect crystal both linear and nonlinear susceptibilities are spatially periodic functions. So it may be expanded into a Fourier series with respect to the reciprocal lattice vectors. Accordingly, as in the linear theory, the electrical field may be presented in the form

$$\tilde{\mathbf{E}}(\mathbf{r}, \omega_q) = \sum_{\mathbf{g}} \tilde{\mathbf{E}}_{\mathbf{g}}(\mathbf{r}, \omega_q) \exp[i\mathbf{k}_{\mathbf{g}}(\omega_q)\mathbf{r}],$$

where $\tilde{\mathbf{E}}_{\mathbf{g}}(\mathbf{r}, \omega_q)$ are slowly varying amplitudes and $\mathbf{k}_{\mathbf{g}}(\omega_q) = \mathbf{k}_0(\omega_q) + \mathbf{g}$, $\mathbf{k}_0(\omega_q)$ are the wavevectors of transmitted waves and \mathbf{g} are reciprocal lattice vectors. If absorption is neglected, $k_0^2(\omega_q) = (\omega_q^2/c^2)[1 + \chi_0^{(1)}(\omega_q)]$, where $\chi_0^{(1)}(\omega_q)$ is the zero-order Fourier component of linear susceptibility. The left-hand side of (4) is the same as in the linear theory and it may be presented in the same form as in the linear theory (Takagi, 1969). Consider the one-beam case of diffraction. Let the incident wave frequency be ω . In this case the third harmonic 3ω is formed. For this process the terms with $\chi_{ijk0}^{(3)}(3\omega; \omega, \omega, \omega)$ are responsible. Here the subscript 0 corresponds to the zero-order Fourier component of the corresponding susceptibility. In the general case the third-order nonlinear susceptibility tensor has 81 elements. In an isotropic medium the number of nonzero elements is 21. Three of them are independent and all elements may be presented in the form

$$\chi_{ijkl}^{(3)} = \chi_{1122}^{(3)} \delta_{ij} \delta_{kl} + \chi_{1212}^{(3)} \delta_{ik} \delta_{jl} + \chi_{1221}^{(3)} \delta_{il} \delta_{jk},\quad (6)$$

where δ_{ij} is the Kronecker delta. In an isotropic medium,

$$\begin{aligned}\chi_{1122}^{(3)}(3\omega; \omega, \omega, \omega, \mathbf{r}) &= \chi_{1212}^{(3)}(3\omega; \omega, \omega, \omega, \mathbf{r}) \\ &= \chi_{1221}^{(3)}(3\omega; \omega, \omega, \omega, \mathbf{r})\end{aligned}$$

and thus

$$\chi_{ijkl}^{(3)}(3\omega; \omega, \omega, \omega, \mathbf{r}) = \chi_{1122}^{(3)}(3\omega; \omega, \omega, \omega, \mathbf{r}) \times (\delta_{ij}\delta_{kl} + \delta_{ik}\delta_{jl} + \delta_{il}\delta_{jk}). \quad (7)$$

Let the propagation direction of the incidence wave be perpendicular to the entrance surface of the crystal (z direction). In the first approximation one may neglect the backward influence of the third harmonic on the amplitude of the incidence wave. According to (4), the wave equation for the third-harmonic slowly varying amplitude will be

$$2i \frac{d\tilde{E}_{0i}(3\omega)}{dz} = -k(3\omega)\chi_{ijkl0}^{(3)}(3\omega; \omega, \omega, \omega)\tilde{E}_{0j}(\omega)\tilde{E}_{0k}(\omega)\tilde{E}_{0l}(\omega) \times \exp\{i[3k(\omega) - k(3\omega)]z\}. \quad (8)$$

On the right-hand side we replaced $k^2(3\omega) \approx (3\omega)^2/c^2$. If the crystalline plate has thickness L , integration of (8) brings the solution

$$\tilde{E}_{0i}(3\omega) = ik(3\omega)\chi_{ijkl0}^{(3)}(3\omega; \omega, \omega, \omega)\tilde{E}_{0j}(\omega)\tilde{E}_{0k}(\omega)\tilde{E}_{0l}(\omega) \times [\exp(i\Delta kL) - 1]/(2\Delta k), \quad (9)$$

where $\Delta k = 3k(\omega) - k(3\omega)$ is the so-called wavevector mismatch. For the intensity from (9) we have

$$I_{0i}(3\omega) = |\tilde{E}_{0i}(3\omega)|^2 = 0.25k^2(3\omega)|\chi_{ijkl0}^{(3)}(3\omega; \omega, \omega, \omega)\tilde{E}_{0j}(\omega)\tilde{E}_{0k}(\omega)\tilde{E}_{0l}(\omega)|^2 L^2 \times \sin^2(\Delta kL/2)/(\Delta kL/2)^2. \quad (10)$$

Since $\Delta k \approx 3k(\omega)|\chi_0^{(1)}(\omega)|/2$, then from (10) it follows that the third-harmonic intensity is small and practically vanishes when $L > 2/\Delta k \approx 4/(3k|\chi_0^{(1)}|) \approx 10 \mu\text{m}$. The main nonlinear process, for which the wavevector mismatch is zero, is the propagation of the main frequency ω in a media with self-induced refractive index. This process is described by the term $\chi_{ijkl}^{(3)}(\omega; \omega, \omega, -\omega, \mathbf{r})$. In an isotropic medium for this choice of frequencies the susceptibility tensor has two independent components and

$$\chi_{ijkl}^{(3)}(\omega; \omega, \omega, -\omega, \mathbf{r}) = \chi_{1122}^{(3)}(\omega; \omega, \omega, -\omega, \mathbf{r})(\delta_{ij}\delta_{kl} + \delta_{ik}\delta_{jl}) + \chi_{1221}^{(3)}(\omega; \omega, \omega, -\omega, \mathbf{r})\delta_{il}\delta_{jk}. \quad (11)$$

According to (5) one finds

$$\tilde{P}_i^{(3)}(\mathbf{r}, \omega) = 3\varepsilon_0\chi_{ijkl}^{(3)}(\omega; \omega, \omega, -\omega, \mathbf{r})\tilde{E}_j(\mathbf{r}, \omega)\tilde{E}_k(\mathbf{r}, \omega)\tilde{E}_l^*(\mathbf{r}, \omega). \quad (12)$$

Using (11) and (12) we find

$$\tilde{\mathbf{P}}^{(3)} = \varepsilon_0 A \tilde{\mathbf{E}}(\tilde{\mathbf{E}}\tilde{\mathbf{E}}^*) + \varepsilon_0 B \tilde{\mathbf{E}}^*(\tilde{\mathbf{E}}\tilde{\mathbf{E}}), \quad (13)$$

where $A = 3\chi_{1122}^{(3)} + 3\chi_{1221}^{(3)}$, $B = 3\chi_{1221}^{(3)}$. According to the classical theory of polarization, $\chi_{1122}^{(3)} = \chi_{1221}^{(3)}$ and $A = 6\chi_{1122}^{(3)}$ (Boyd, 2003). The classical theory of polarization brings the following expression,

$$\chi_{ijkl}^{(3)}(\omega; \omega, \omega, -\omega, \mathbf{r}) = \chi^{(3)}(\omega, \mathbf{r}) \frac{(\delta_{ij}\delta_{kl} + \delta_{ik}\delta_{jl} + \delta_{il}\delta_{jk})}{3}, \quad (14)$$

where, when the frequency of incident radiation is larger than the resonance frequencies, $\chi^{(3)}(\omega, \mathbf{r}) = n(\mathbf{r})e^4b/(\varepsilon_0m^3\omega^8) > 0$, $n(\mathbf{r})$ is the concentration of electrons, e and m are the electron charge and mass, and b is a phenomenological constant to which is proportional the third-order nonlinear restoring force. Recall that the linear susceptibility $\chi^{(1)}(\omega, \mathbf{r}) = -n(\mathbf{r})e^2/(\varepsilon_0m\omega^2)$. Formula (14) shows that the sign of the third-order susceptibility is positive and so its phase is shifted by π with respect to the linear susceptibility. According to the quantum-mechanical theory of polarization due to two-photon processes, $\chi_{1122}^{(3)} \neq \chi_{1221}^{(3)}$. The quantum-mechanical calculation of third-order susceptibility, using the dipole approximation, is given by Boyd [2003; formulas (4.312)–(4.314)]. Using, in the formula of $\chi_{1122}^{(3)}$ [formula (4.314) of Boyd (2003)], only one-photon processes terms [the second term in (4.314)] and taking into account that for X-rays the frequency ω is larger than the resonance frequencies of electrons (neglecting the resonance frequencies), the following estimate, according to (14), may be obtained,

$$\chi^{(3)} \approx \frac{n(\mathbf{r})e^4a_0^4}{\varepsilon_0\hbar^3\omega^3}, \quad (15)$$

and $\chi_{1122}^{(3)} = \chi_{1221}^{(3)} \equiv \chi^{(3)}/3$, $A = 2\chi^{(3)}$, $B = A/2$. In (14), $a_0 = 5.3 \times 10^{-11} \text{ m}$ is the Bohr radius. It is convenient to introduce $\eta^{(3)} = A + B$. Using the approximation (14) we have $\eta^{(3)} = 3\chi^{(3)}$. Using the values $n(\mathbf{r}) \approx 10^{28}\text{--}10^{30} \text{ m}^{-3}$ and $\omega \approx 10^{19} \text{ s}^{-1}$, from (15) the following estimate is obtained: $\chi^{(3)}(\omega, \mathbf{r}) \approx 10^{-31}\text{--}10^{-33} \text{ m}^2 \text{ V}^{-2}$. For elements with low atomic number $Z < 10$, Zambianchi (2003) obtained the estimate $\chi^{(3)} \approx 2 \times 10^{-40} \text{ m}^2 \text{ V}^{-2}$. This estimate is less than that predicted in this article by nine orders. Zambianchi (2003) concluded that the nonlinear scattering by bound electrons is not essential. Our estimate shows that this scattering may be essential. Let us denote $|\chi^{(1)}|/\chi^{(3)} = E_{\text{cr}}^2 = I_{\text{cr}}$, where E_{cr} is the critical strength of the electrical field for which the contribution of the nonlinear part of scattering equals that of the linear one and I_{cr} is the corresponding intensity. Using (15) and $\chi^{(1)}(\omega, \mathbf{r}) = -n(\mathbf{r})e^2/(\varepsilon_0m\omega^2)$ we have $E_{\text{cr}} = [\hbar^3\omega/(me^2a^4)]^{1/2} \approx 1.2 \times 10^{13} \text{ V m}^{-1}$.

Now, using (4) and the same technique as in the linear case (Takagi, 1969), the third-order nonlinear Takagi's equations may be obtained (Balyan, 2015). As may be shown, in the two-wave diffraction case, if the incident beam is σ - or π -polarized, in the crystal the corresponding equations may be separated, so that only σ - or π -polarized waves in the crystal propagate, respectively. But when the incidence beam has both σ - and π -polarized components, their equations may not be separated due to nonlinear terms in the wave equation. Let us present the fields in the form $\tilde{\mathbf{E}}(\mathbf{r}, \omega) = \tilde{\mathbf{E}}_0(\mathbf{r}, \omega)\exp[i\mathbf{K}_0(\omega)\mathbf{r}] + \tilde{\mathbf{E}}_h(\mathbf{r}, \omega)\exp[i\mathbf{K}_h(\omega)\mathbf{r}]$. Here the wavevectors are chosen so that they satisfy the exact Bragg condition $\mathbf{K}_0^2 = \mathbf{K}_h^2 = k^2 = (2\pi/\lambda)^2$, where λ is the wavelength. As may be shown, using (4), the third-order nonlinear Takagi's equations for the two-beam diffraction case and for σ -polarization have the form

$$\begin{aligned} & \frac{2i}{k} \frac{\partial E_0}{\partial s_0} + \left[\eta_0^{(3)} (|E_0|^2 + |E_h|^2) \right. \\ & \quad \left. + \eta_h^{(3)} E_0 E_h^* + \eta_h^{(3)} E_0^* E_h \right] \exp(-\mu x / \cos \theta) E_0 \\ & \quad + \left\{ \chi_h^{(1)} + \left[\eta_0^{(3)} E_0 E_h^* + \eta_h^{(3)} (|E_0|^2 + |E_h|^2) \right. \right. \\ & \quad \left. \left. + \eta_{2h}^{(3)} E_0^* E_h \right] \exp(-\mu x / \cos \theta) \right\} E_h = 0, \end{aligned} \tag{16}$$

$$\begin{aligned} & \frac{2i}{k} \frac{\partial E_h}{\partial s_h} + \left[\eta_0^{(3)} (|E_0|^2 + |E_h|^2) \right. \\ & \quad \left. + \eta_h^{(3)} E_0 E_h^* + \eta_h^{(3)} E_0^* E_h \right] \exp(-\mu x / \cos \theta) E_h \\ & \quad + \left\{ \chi_h^{(1)} + \left[\eta_0^{(3)} E_0^* E_h + \eta_h^{(3)} (|E_0|^2 + |E_h|^2) \right. \right. \\ & \quad \left. \left. + \eta_{2h}^{(3)} E_0 E_h^* \right] \exp(-\mu x / \cos \theta) \right\} E_0 = 0, \end{aligned}$$

where $E_{0,h} = \tilde{E}_{0,h} \exp[-ik\chi_0^{(1)}x/(2\cos\theta)]$, $\mu = k\chi_{0i}^{(1)}$ is the crystal linear absorption coefficient, the x axis is oriented along the reflecting planes, the z axis is oriented anti-parallel to the diffraction vector \mathbf{h} inward the crystal, and s_0 and s_h are coordinates along the propagation directions of the transmitted and diffracted waves, respectively. Here, $\chi_h^{(1)}$ is the Fourier coefficient of linear susceptibility for diffraction vector \mathbf{h} , and $\eta_{0,h,2h}^{(3)}$ is the corresponding Fourier coefficient of the third-order nonlinear part of the susceptibility.

3. Analytical consideration

Let us consider the third-order nonlinear two-wave symmetric Bragg-case dynamical diffraction of a σ -polarized plane monochromatic wave in a perfect crystal. On the entrance surface $z = 0$ the electrical field of the incidence wave is

$$E^{(i)}(x, 0) = E_0^{(i)} \exp(ik \sin \theta^{(i)} x), \tag{17}$$

where $E_0^{(i)}$ is the constant amplitude and $\theta^{(i)}$ is the angle between the propagation direction of the incidence wave and the reflecting planes (which are parallel to the entrance surface). Let us denote $\Delta\theta = \theta^{(i)} - \theta$ as the deviation from the exact Bragg angle θ . In the case of a plane wave and in a non-absorbing crystal, the amplitudes E_0 and E_h of the transmitted and reflected waves, respectively, can be presented in the form

$$E_{0,h} = F_{0,h}(z) \exp(ipx), \tag{18}$$

where p is a parameter and must be found from the boundary conditions. The boundary conditions on the entrance ($z = 0$) and exit ($z = T$) surfaces are the same as in the linear theory (Authier, 2001; Pinsker, 1982),

$$\begin{aligned} E_0(x, 0) &= E_0^{(i)} \exp(ik \cos \theta \Delta\theta x), \\ E_h(x, T) &= 0. \end{aligned} \tag{19}$$

From (17)–(19) it follows

$$\begin{aligned} F_0(0) &= E_0^{(i)}, & F_h(T) &= 0, \\ p &= -k \sin \theta \left(\Delta\theta + \frac{\chi_0^{(1)}}{\sin 2\theta} \right). \end{aligned} \tag{20}$$

Inserting (18) into nonlinear Takagi's equations (16), the propagation equations for $F_{0,h}$ can be written as

$$\begin{aligned} & 2ik \sin \theta \frac{dF_0}{dz} - 2kp \cos \theta F_0 \\ & \quad + k^2 \left[\eta_0^{(3)} (|F_0|^2 + |F_h|^2) + \eta_h^{(3)} F_0 F_h^* + \eta_h^{(3)} F_0^* F_h \right] F_0 \\ & \quad + k^2 \left[\chi_h^{(1)} + \eta_0^{(3)} F_0 F_h^* + \eta_h^{(3)} (|F_0|^2 + |F_h|^2) + \eta_{2h}^{(3)} F_0^* F_h \right] F_h = 0, \\ & -2ik \sin \theta \frac{dF_h}{dz} - 2kp \cos \theta F_h \\ & \quad + k^2 \left[\eta_0^{(3)} (|F_0|^2 + |F_h|^2) + \eta_h^{(3)} F_0 F_h^* + \eta_h^{(3)} F_0^* F_h \right] F_h \\ & \quad + k^2 \left[\chi_h^{(1)} + \eta_0^{(3)} F_0^* F_h + \eta_h^{(3)} (|F_0|^2 + |F_h|^2) + \eta_{2h}^{(3)} F_0 F_h^* \right] F_0 = 0. \end{aligned} \tag{21}$$

For an absorbing crystal, the susceptibility is a complex quantity, the imaginary part of which is connected to absorption in the crystal. In a non-absorbing crystal, both for linear and nonlinear parts of the susceptibilities, the Fourier coefficients for any vector of diffraction are complex conjugated with the Fourier coefficient for the diffraction vector of the opposite sign, $\chi_h^* = \chi_{\bar{h}}$, $\eta_{h,2h}^* = \eta_{\bar{h},2\bar{h}}$. In this case two integrals of motion can be found. The first is obtained by multiplying the first and the second equations of (21) by F_0^* and F_h^* , the first and the second equations of the complex conjugate system of (21) by $-F_0$ and $-F_h$ and summing the obtained four equations. The second is obtained by multiplying the first and the second equations of (21) by dF_0^*/dz and dF_h^*/dz , respectively, the first and the second equations of the complex conjugate of (21) by dF_0/dz and dF_h/dz , respectively, and summing up the four obtained equations. The two integrals of motions are

$$\begin{aligned} & |F_0(z)|^2 - |F_h(z)|^2 = \text{constant} = C_1, \\ & -2kp \cos \theta I + 2k^2 \text{Re}[\chi_h^{(1)} F_0 F_h^*] \\ & \quad + k^2 \frac{\eta_0^{(3)}}{2} (I^2 + 2|F_0|^2 |F_h|^2) + 2k^2 \text{Re}[\eta_h^{(3)} I F_0 F_h^*] \\ & \quad + k^2 \text{Re}[\eta_{2h}^{(3)} F_0^2 F_h^{*2}] = \text{constant} = C_2. \end{aligned} \tag{22}$$

Here $I = |F_0|^2 + |F_h|^2$.

Let us provide an analytical analysis of nonlinear diffraction in a non-absorbing crystal, using propagation equations (21) and integrals of motion (22). One can represent the solutions in the complex form

$$F_{0,h}(z) = \rho_{0,h}(z) \exp[i\varphi_{0,h}(z)]. \tag{23}$$

Inserting (23) into (21) and separating the real and imaginary parts, one finds

$$2k \sin \theta \frac{d\varphi_0}{dz} + 2kp \cos \theta - k^2 \eta_0^{(3)} (\rho_0^2 + 2\rho_h^2) + 2k^2 \rho_h \rho_0 |\eta_h^{(3)}| \cos(\gamma + \delta_h^{(1)}) - k^2 (|\chi_h^{(1)}| - |\eta_h^{(3)}| I) \cos(\gamma + \delta_h^{(1)}) \frac{\rho_h}{\rho_0} + k^2 |\eta_{2h}^{(3)}| \rho_h^2 \cos(2\gamma + \delta_{2h}^{(1)}) = 0,$$

$$2k \sin \theta \frac{d\rho_0}{dz} - k^2 \rho_h (|\chi_h^{(1)}| - |\eta_h^{(3)}| I) \sin(\gamma + \delta_h^{(1)}) + k^2 |\eta_{2h}^{(3)}| \rho_0 \rho_h^2 \sin(2\gamma + \delta_{2h}^{(1)}) = 0, \quad (24)$$

$$2k \sin \theta \frac{d\rho_h}{dz} - 2kp \cos \theta + k^2 \eta_0^{(3)} (2\rho_0^2 + \rho_h^2) - 2k^2 |\eta_h^{(3)}| \rho_0 \rho_h \cos(\gamma + \delta_h^{(1)}) + k^2 (|\chi_h^{(1)}| - |\eta_h^{(3)}| I) \cos(\gamma + \delta_h^{(1)}) \frac{\rho_0}{\rho_h} - k^2 |\eta_{2h}^{(3)}| \rho_0^2 \cos(2\gamma + \delta_{2h}^{(1)}) = 0,$$

$$2k \sin \theta \frac{d\rho_h}{dz} - k^2 \rho_0 (|\chi_h^{(1)}| - |\eta_h^{(3)}| I) \sin(\gamma + \delta_h^{(1)}) + k^2 |\eta_{2h}^{(3)}| \rho_0^2 \rho_h \sin(2\gamma + \delta_{2h}^{(1)}) = 0.$$

In (24), $\gamma(z) = \varphi_0(z) - \varphi_h(z)$, $\delta_h^{(1)}$ and $\delta_{2h}^{(1)}$ are the phases of $\chi_h^{(1)}$ and $\chi_{2h}^{(1)}$, respectively. In (24), we take into account that the phases of $\eta_h^{(3)}$ and $\eta_{2h}^{(3)}$ are shifted relative to the phases of $\chi_h^{(1)}$ and $\chi_{2h}^{(1)}$, respectively, by π . Inserting (23) into (22), the integrals of motion can be rewritten in the form

$$\rho_0^2 - \rho_h^2 = C_1, \quad (25)$$

$$-2kp \cos \theta I + 2k^2 (|\chi_h^{(1)}| - I |\eta_h^{(3)}|) \rho_0 \rho_h \cos(\gamma + \delta_h^{(1)}) + k^2 \frac{\eta_0^{(3)}}{2} (I^2 + 2\rho_0^2 \rho_h^2) - k^2 |\eta_{2h}^{(3)}| \rho_0^2 \rho_h^2 \cos(2\gamma + \delta_{2h}^{(1)}) = C_2.$$

Using boundary conditions (20), it is not difficult to show that

$$0 \leq C_1 < I^{(i)} = |E_0^{(i)}|^2, \quad (26)$$

$$C_2 = -2pk \cos \theta C_1 + k^2 \frac{\eta_0^{(3)}}{2} C_1^2.$$

Further analytical consideration can be made for forbidden reflection **2h**. In this case, using the second equations of (25) and (26), one finds

$$\cos(\gamma + \delta_h^{(1)}) = \frac{(4p \cos \theta - 3k \rho_0^2 \eta_0^{(3)}) \rho_h}{2k (|\chi_h^{(1)}| - I |\eta_h^{(3)}|) \rho_0}. \quad (27)$$

From (27),

$$\sin(\gamma + \delta_h^{(1)}) = \pm \left[1 - \cos^2(\gamma + \delta_h^{(1)}) \right]^{1/2} = \pm \frac{\left[4k^2 (|\chi_h^{(1)}| - I |\eta_h^{(3)}|)^2 \rho_0^2 - (4p \cos \theta - 3k \rho_0^2 \eta_0^{(3)})^2 \rho_h^2 \right]^{1/2}}{2k (|\chi_h^{(1)}| - I |\eta_h^{(3)}|) \rho_0}. \quad (28)$$

Inserting (28) into (24) brings

$$4 \sin \theta \frac{d\rho_0}{dz} \mp \frac{\rho_h}{\rho_0} \left[4k^2 (|\chi_h^{(1)}| - I |\eta_h^{(3)}|)^2 \rho_0^2 - (4p \cos \theta - 3k \rho_0^2 \eta_0^{(3)})^2 \rho_h^2 \right]^{1/2} = 0, \quad (29)$$

$$4 \sin \theta \frac{d\rho_h}{dz} \mp \left[4k^2 (|\chi_h^{(1)}| - I |\eta_h^{(3)}|)^2 \rho_0^2 - (4p \cos \theta - 3k \rho_0^2 \eta_0^{(3)})^2 \rho_h^2 \right]^{1/2} = 0.$$

Using in (29) the first integral of motion (25) one obtains separate equations for $\rho_{0,h}$,

$$4 \sin \theta \rho_0 \frac{d\rho_0}{dz} \mp (\rho_0^2 - C_1)^{1/2} \left[4k^2 (|\chi_h^{(1)}| - (2\rho_0^2 - C_1) |\eta_h^{(3)}|)^2 \rho_0^2 - (4p \cos \theta - 3k \rho_0^2 \eta_0^{(3)})^2 (\rho_0^2 - C_1) \right]^{1/2} = 0, \quad (30)$$

$$4 \sin \theta \frac{d\rho_h}{dz} \mp \left[4k^2 (|\chi_h^{(1)}| - (2\rho_h^2 + C_1) |\eta_h^{(3)}|)^2 (\rho_h^2 + C_1) - (4p \cos \theta - 3k(\rho_h^2 + C_1) \eta_0^{(3)})^2 \rho_h^2 \right]^{1/2} = 0.$$

The solutions of (30) can be presented *via* elliptic functions, but it is necessary to have analytic expressions of roots of expressions in square-roots of (30). This fact makes further analytical consideration very difficult. Further analytical consideration can be made in the total reflection region. According to the first integral of motions (25), in this case $C_1 = 0$ and, according to (26), $C_2 = 0$ as well. Besides, the two equations of (30) become identical. Both equations, after multiplying by $\rho_{0,h}$, can be rewritten as

$$2 \sin \theta \frac{d\rho_{0,h}^2}{dz} + \rho_{0,h}^2 \left[4k^2 (|\chi_h^{(1)}| - 2\rho_{0,h}^2 |\eta_h^{(3)}|)^2 - (4p \cos \theta - 3k \rho_{0,h}^2 \eta_0^{(3)})^2 \right]^{1/2} = 0. \quad (31)$$

We take the sign ‘+’ since in the total reflection region the amplitudes must decrease in the crystal. A real solution can take place if the expressions in the square-roots are positive. This requirement is compatible with boundary conditions on the exit and entrance surfaces if

$$4|p| \cos \theta < 2k|\chi_h^{(1)}|, \quad (32)$$

$$\left[2k|\chi_h^{(1)}| - 4p \cos \theta + (3\eta_0^{(3)} - 4k|\eta_h^{(3)}|)I^{(i)} \right] \times \left[2k|\chi_h^{(1)}| + 4p \cos \theta - (3\eta_0^{(3)} + 4k|\eta_h^{(3)}|)I^{(i)} \right] > 0.$$

From the first equation of (32) it follows that $2k|\chi_h^{(1)}| \pm 4p \cos \theta > 0$, which is the condition of total reflection in linear theory. If $3\eta_0^{(3)} > 4|\eta_h^{(3)}|$, which usually occurs, the condition of total reflection, according to (32), is

$$-2k|\chi_h^{(1)}| + k(3\eta_0^{(3)} + 4|\eta_h^{(3)}|)I^{(i)} < 4p \cos \theta < 2k|\chi_h^{(1)}|. \quad (33)$$

As follows from (33), the centre of the total reflection region is not at $p = 0$, as in the linear theory, but is

$$p_c = \frac{k(3\eta_0^{(3)} + 4|\eta_h^{(3)}|)I^{(i)}}{8 \cos \theta} \quad (34)$$

and is a function of the intensity of the incidence wave. According to (33), the width of the total reflection region is

$$\Delta p = \frac{4k|\chi_h^{(1)}| - k(3\eta_0^{(3)} + 4|\eta_h^{(3)}|)I^{(i)}}{4 \cos \theta}. \quad (35)$$

The width of the nonlinear total reflection region is less than that in linear theory and is a function of the intensity of the incidence wave. According to (35), the width of the total reflection region is equal to zero for the intensity $I_{\max}^{(i)}$ when $4|\chi_h^{(1)}| = (3\eta_0^{(3)} + 4|\eta_h^{(3)}|)I_{\max}^{(i)}$. For intensities $I^{(i)} > I_{\max}^{(i)}$, when $4|\chi_h^{(1)}| < (3\eta_0^{(3)} + 4|\eta_h^{(3)}|)I^{(i)}$, the total reflection region in nonlinear theory is absent. Let us introduce the deviation parameter $y = \sin 2\theta(\Delta\theta + \chi_0^{(1)}/\sin 2\theta)/|\chi_h^{(1)}|$ (for a non-absorbing crystal it is a real quantity). Using the definition of p [see (20)], from (33)–(35) it is not difficult to find the total reflection region condition, the total reflection centre coordinate and the width of the total reflection region in terms of the parameter y ,

$$-1 < y < 1 - \frac{(3\eta_0^{(3)} + 4|\eta_h^{(3)}|)I^{(i)}}{2|\chi_h^{(1)}|},$$

$$y_c = -\frac{(3\eta_0^{(3)} + 4|\eta_h^{(3)}|)I^{(i)}}{4|\chi_h^{(1)}|}, \quad (36)$$

$$\Delta y = 2 - \frac{(3\eta_0^{(3)} + 4|\eta_h^{(3)}|)I^{(i)}}{2|\chi_h^{(1)}|}.$$

As may be seen from (36), the left bound $y_{\min} = -1$ of the total reflection region is the same as in the linear theory and does not depend on the intensity of the incidence wave. The right bound $y_{\max} = 1 - (3\eta_0^{(3)} + 4|\eta_h^{(3)}|)I^{(i)}/(2|\chi_h^{(1)}|)$ is a function of the intensity of the incidence wave and linearly decreases with increasing intensity. The centre y_c is shifted to the direction of negative y (to the direction of low angles). The width $\Delta y = y_{\max} - y_{\min}$ is less than in the linear theory and decreases with increasing intensity. As mentioned above, for $I^{(i)} > I_{\max}^{(i)}$ there is no total reflection region in the nonlinear theory. These rocking-curve behaviors may be explained on the basis of the

propagation equations (29). As may be seen from (29), instead of the deviation parameter p an effective self-induced nonlinear deviation parameter $p_{\text{eff}} = p - 3k\rho_0^2\eta_0^{(3)}/(4\cos\theta)$ appears and $\chi_h^{(1)}$ is replaced by a self-induced effective one $\chi_{\text{heff}} = |\chi_h^{(1)}| - 2\rho_{0,h}^2|\eta_h^{(3)}|$. This means that during propagation the beam changes its deviation from the Bragg exact direction depending on the intensity. The ‘-’ sign is due to the relative phase shift by π linear and nonlinear parts of the susceptibility (phase mismatch of the linear and nonlinear parts). As seen from the definition of p [formula (20)], $\Delta\theta$ is replaced by an effective one, $\Delta\theta_{\text{eff}} = \Delta\theta + 3\rho_0^2\eta_0^{(3)}/(2\sin 2\theta)$. Thus for positive $\Delta\theta + \chi_{0r}^{(1)}/\sin 2\theta$ (i.e. for positive y), the effective deviation parameter increases and the beam reflection reduces; meanwhile, for negative $\Delta\theta + \chi_{0r}^{(1)}/\sin 2\theta$ the absolute value of the effective deviation parameter may decrease and the beam reflection is not disturbed. The expression for χ_{heff} shows that the increasing intensity brings about a decreasing of the scattering in the diffraction direction. These features alternatively may be explained considering constant $\Delta\theta$ but effective self-induced $\chi_{0\text{eff}} = \chi_0^{(1)} + 3\rho_0^2\eta_0^{(3)}/2$ and $\chi_{\text{heff}} = |\chi_h^{(1)}| - 2\rho_{0,h}^2|\eta_h^{(3)}|$. It is interesting that $\chi_{\text{heff}} = 0$ when $|\chi_h^{(1)}| = 2\rho_{0,h}^2|\eta_h^{(3)}|$.

Let us solve propagation equation (31) for the reflected wave in the total reflection region. It is not difficult to see that

$$\int \frac{d\rho_{0,h}^2}{\rho_{0,h}^2(a\rho_h^4 + b\rho_{0,h}^2 + c_1)^{1/2}} = -\frac{z}{2\sin\theta} + \text{constant}, \quad (37)$$

where

$$a = k^2(16|\eta_h^{(3)}|^2 - 9\eta_0^{(3)2}),$$

$$b = -4k^2|\chi_h^{(1)}|(3y\eta_0^{(3)} + 4|\eta_h^{(3)}|), \quad (38)$$

$$c_1 = 4k^2|\chi_h^{(1)}|^2(1 - y^2).$$

According to the first condition of (36), $c_1 > 0$. Using a tabular integral (Prudnikov *et al.*, 1986), from (37) one finds

$$\ln \frac{|2c_1 + b\rho_h^2 + 2[c_1(a\rho_h^4 + b\rho_h^2 + c_1)]^{1/2}}{C_3\rho_h^2} = \frac{\sqrt{c_1}z}{2\sin\theta}, \quad (39)$$

where C_3 is a constant. As may be seen, the solution (39) in the total reflection region is possible only for a semi-infinite crystal, since $\rho_h^2 = 0$ when $z = T$. Using the boundary condition on the entrance surface $\rho_h^2(0) = I^{(i)}$, from (39) one finds $C_3 = |2c_1 + bI^{(i)} + 2[c_1(aI^{(i)2} + bI^{(i)} + c_1)]^{1/2}|/I^{(i)}$. From (39) we have the following solution as well,

$$\rho_h^2 = \pm \frac{4C_3c_1 \exp(\sqrt{c_1}z/2\sin\theta)}{[\pm C_3 \exp(\sqrt{c_1}z/2\sin\theta) - b]^2 - 4c_1a}. \quad (40)$$

Since $3\eta_0^{(3)} > 4|\eta_h^{(3)}|$ and from definition of a [see (38)] it follows that $a < 0$. Therefore in (40) the ‘+’ sign must be taken and finally we find

$$\rho_h^2 = \frac{4C_3c_1 \exp(-z/\tau)}{[C_3 - b \exp(-z/\tau)]^2 - 4ac_1 \exp(-2z/\tau)}, \quad (41)$$

where $\tau = 2\sin\theta/\sqrt{c_1}$ coincides with the extinction depth in linear theory (Authier, 2001). As seen from (41), for $z/\tau \gg 1$ the intensity of the reflected wave exponentially tends to zero,

$$\rho_h^2 = \frac{4c_1 \exp(-z/\tau)}{C_3}. \quad (42)$$

Since $C_1 = 0$, from (9) the same dependence (25) of ρ_0^2 on z follows. Note that c_1 is the same both in linear and nonlinear theories and in the linear theory $a = b = 0$. By taking $a = b = 0$ in (41) one obtains the solution of the linear theory (Authier, 2001).

Fig. 1 [according to (36)] depicts the dependence of the left (curve 1) and right (curve 2) bounds $y_{\min, \max}$ of the total reflection region on the intensity of the incidence wave according to nonlinear theory. Curve 3 is the right bound according to linear theory (the left bounds both in linear and nonlinear theories are the same and do not depend on the intensity of the incidence wave). For the nonlinear part the relations $\eta_0^{(3)} = 3|\chi_0^{(1)}|/I_{cr}$, $\eta_h^{(3)} = 3|\chi_h^{(1)}|/I_{cr}$ are used. Accordingly, the intensities are given in units $I_{cr}/3$. The necessary values of the linear part of the susceptibility are taken from Pinsker (1982) for reflection Si(111) [for which the reflection Si(222) is forbidden]. The radiation wavelength is $\lambda = 0.71 \text{ \AA}$ (17.46 keV). The left bounds $y_{\min} = -1$ both in linear and nonlinear theories do not depend on the intensity and are the same; the right bound y_{\max} in linear theory also does not depend on the intensity but the right bound in nonlinear theory linearly decreases with increasing intensity. For the value of the intensity $I^{(i)} = I_{\max}^{(i)} \approx 0.42$, the right and left bounds in nonlinear theory coincide and the width of the total reflection region equals zero. For the intensities $I^{(i)} > I_{\max}^{(i)}$ there is no total reflection region. In Fig. 2, according to (36), the dependence of the total reflection region width on the intensity of the incidence wave is presented. The width is negative for $I^{(i)} > I_{\max}^{(i)}$ and equal to zero for $I^{(i)} = I_{\max}^{(i)}$. Based on (36), Fig. 3 presents the dependence of the centre of the total reflection region on the intensity of the incidence wave for $0 < I^{(i)} \leq I_{\max}^{(i)}$. Using (41), in Fig. 4 the dependence of $\rho_h^2/I^{(i)}$ on z for $I^{(i)} = 0.2, 0.4$ (curves 2 and 3, respectively) are presented. The same dependence in linear theory (curve 1) is

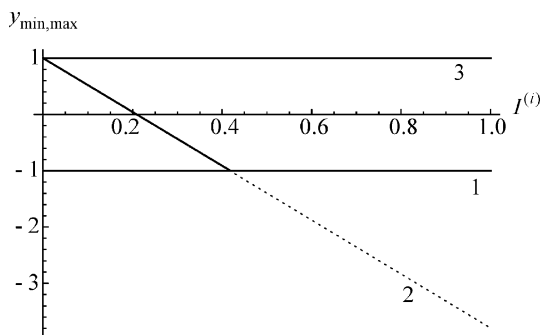


Figure 1 Dependences of the left and right bounds y_{\min} and y_{\max} of the total reflection regions of linear and nonlinear diffractions on the intensity of the incidence wave $I^{(i)}$ according to formula (36) (non-absorbing crystal). 1: the left bounds of the rocking curves according to linear and nonlinear theories are the same; 2: the right bound according to nonlinear theory; 3: the right bound according to linear theory. The dashed line part of curve 2 corresponds to intensities for which the total reflection region does not exist.

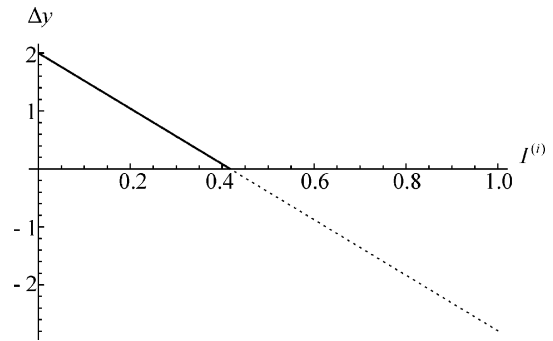


Figure 2 Dependence of the width Δy of the total reflection region on the intensity $I^{(i)}$ of the incidence wave in nonlinear theory according to formula (36) (non-absorbing crystal). The dashed line part of the curve 2 corresponds to intensities for which the total reflection region does not exist.

presented as well. Each of these curves are presented for the corresponding values y_c and $y_c(0.2) = -0.48$, $y_c(0.4) = -0.96$, and in linear theory $y_c = 0$. The depth is given in units of $\tau_0 = \sin \theta / (k|\chi_h^{(1)}|)$, which is the extinction depth in linear theory at the centre of the total reflection region (Authier, 2001). For large depths, according to (42), the extinction depth $\tau(-0.48)/\tau_0 = 1.14$ for $I^{(i)} = 0.2$ and $\tau(-0.96)/\tau_0 = 3.57$ for $I^{(i)} = 0.4$; meanwhile $\tau_0 = 0.75 \mu\text{m}$.

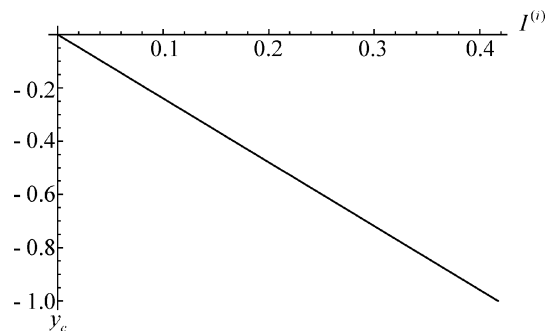


Figure 3 Dependence of the centre y_c of the total reflection region on the intensity of the incidence wave $I^{(i)}$ in nonlinear theory according to formula (36) (non-absorbing crystal).

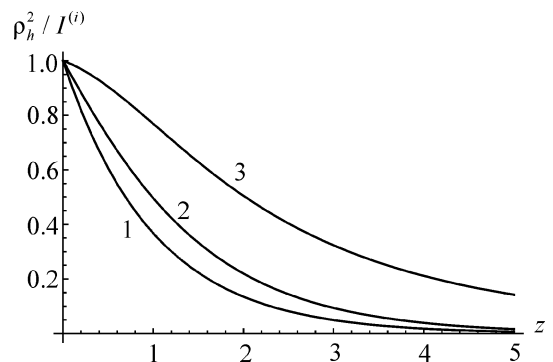


Figure 4 Dependence of the intensity of the reflected wave $\rho_h^2/I^{(i)}$ on depth z in linear (curve 1) and nonlinear theories (curve 2, $I^{(i)} = 0.2$; curve 3, $I^{(i)} = 0.4$) according to formula (41) (non-absorbing crystal).

4. Results of numerical calculations

Despite the analytical consideration being possible only for certain conditions of diffraction, the main features of nonlinear diffraction are investigated. For the general case, numerical calculations must be provided. For obtaining rocking curves in the general case, the numerical method of ‘shooting’ can be used to solve equations (21) or (29) as a boundary value problem. But, as the calculations show, in the nonlinear case this method does not provide solutions of equations (21) or (29). In the nonlinear case it is more convenient to use numerical calculations of nonlinear Takagi’s equations (16). The use of nonlinear Takagi’s equations requires consideration of an incidence wave with spatially restricted size in the diffraction plane (an incidence beam). As shown by the calculations, for obtaining the rocking curve of plane wave linear theory, Takagi’s linear equations must be numerically solved for a beam with size along the entrance surface of more than 20 linear extinction lengths. This is due to diffraction effects at the edges of the beam, which are not essential for a beam with a width which is sufficiently large compared with the linear extinction length. If the rocking curve is created using 40 points in the region $-2 \leq y_r \leq 2$ ($y_r = \text{Re}[y]$) in the nonlinear case, this requires very large computational time. This is why below are presented the results of numerical calculations of nonlinear Takagi’s equations for a beam with a width of 5 linear extinction lengths along the entrance surface. For comparison will be presented the rocking curve of linear plane-wave theory (Authier, 2001) and numerically calculated rocking curve according to linear theory for a beam of the same width. The nonlinear Takagi’s equations can be solved numerically using the well known, in linear theory, half-step algorithm (Authier, 2001; Epelboin, 1977). In the nonlinear case, however, the susceptibility Fourier coefficients effectively are functions of the amplitudes of the waves, and in the nonlinear case, using the same algorithm for obtaining the amplitudes at the exit of any layer, the calculated values of amplitudes on the entrance surface of the same layer can be used for calculation of effective Fourier coefficients of nonlinear theory.

In Fig. 5 the numerically calculated rocking curves for a semi-infinite absorbing crystal depending on the parameter $y_r = \text{Re}[y] = \sin 2\theta(\Delta\theta + \chi_{0r}^{(1)}/\sin 2\theta)/|\chi_h^{(1)}|$ for the same wavelength and reflection as in §3 are presented. Since we consider a beam with a restricted size (5 linear extinction lengths) in the diffraction plane, the rocking curve is the dependence of the integral reflection coefficient,

$$R_h(y_r) = \frac{\int_{-a_1}^{a_1} \exp(-\mu'x/\cos\theta) I_h(x, 0, y_r) dx}{2a_1 I^i}, \quad (43)$$

on y_r . Here, $I_h(x, 0, y_r) = |E_h(x, 0, y_r)|^2$, $\mu' = \mu\Lambda^L$, $\mu = k\chi_{0i}^{(1)}$ is the linear absorption coefficient, $\Lambda^L = \lambda \cos\theta/|\chi_{hr}^{(1)}|$ is the extinction length of linear theory, $2a_1$ is the size of the beam along the entrance surface of the crystal, and the coordinate x along the entrance surface of the crystal is given in units of extinction length of linear theory. The values of Fourier

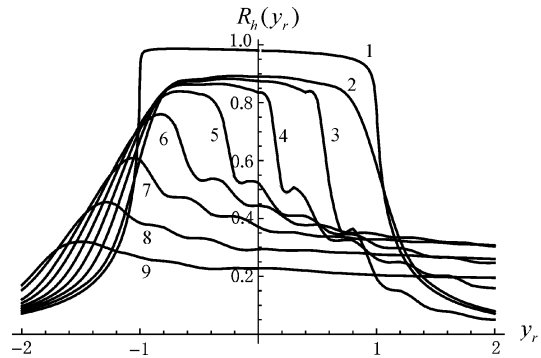


Figure 5 Numerically calculated rocking curves $R_h(y_r)$ [formula (43)] on deviation parameter y_r for various values of the intensity of the incidence wave $I^i = 0.1$ – 0.7 with step 0.1 (curves 3–9, respectively) according to nonlinear theory (the width of the beam is 5 linear extinction lengths). The rocking curve of linear theory (numerical calculation) for a beam of the same width (curve 2) and the rocking curve according to standard plane wave linear dynamical diffraction theory (curve 1) are shown as well. Absorbing crystal.

coefficients of linear theory are taken from Pinsker (1982); for the real parts of Fourier coefficients of nonlinear susceptibility the relations $\eta_{0r}^{(3)} = 3|\chi_{0r}^{(1)}|/I_{cr}$, $\eta_{hr}^{(3)} = 3|\chi_{hr}^{(1)}|/I_{cr}$ are used and for the imaginary parts of the third-order nonlinear susceptibility $\eta_{0,hi}^{(3)}/\eta_{0,hr}^{(3)} = 0.01$ values are taken, which are almost equal to the same ratio of the linear part. Curve 1 is the rocking curve of the exact plane-wave linear theory (Authier, 2001; Pinsker, 1982). Curve 2 is the numerically calculated linear theory rocking curve for the beam with width 5 extinction lengths of the linear theory. Rocking curves 3–9 correspond to numerical-calculated nonlinear rocking curves for intensity values 0.1 – 0.7 with 0.1 step. The behaviours of the nonlinear rocking curves correspond to predictions of analytical consideration [formula (36)]. With increasing intensity the total reflection regions are shifted to the direction of negative y_r and the size of the total reflection region decreases. For intensities above 0.42 the total reflection region does not exist. The intensities of the rocking curves decrease with increasing intensity of the incidence beam. For the intensities for which the total reflection region exists, this is due to the restricted size of the incidence wave. As can be seen from Fig. 5, the slopes of the rocking curves in one side from the centre of the total reflection region and on the opposite side have different behaviours. In the linear case they have almost the same behaviour (the absorption is sufficiently low). The slope from the positive side of y_r due to the effective susceptibility behaviour is more sensitive to nonlinearity and restricted size of the incidence beam. In Fig. 6 the dependence of the intensity

$$I_h'(0, z, y_r) = I_h(0, z, y_r) / I^i \quad (44)$$

of the reflected wave at the centre of the reflected beam ($x = 0$) on z for $I^i = 0.4$ and for three values $y_r = -1.5$ (curve 1), $y_r = y_c(0.4) = -0.959$ (curve 2) and $y_r = 1.5$ (curve 3) are shown. The depth is given in units of $\Lambda^L \tan\theta$. As may be seen for $y_c(0.4)$, the behaviour of the intensity as a function of z is close

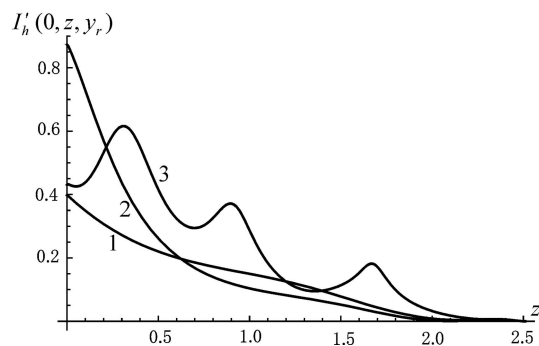


Figure 6 Dependence of the intensity $I'_h(0, z, y_r)$ of the reflected wave [formula (44)] on depth z according to nonlinear theory for various values of y_r : $y_r = -1.5$ (curve 1), $y_r = y_c(0.4) = -0.959$ (curve 2) and $y_r = 1.5$ (curve 3). Absorbing crystal; the width of the beam is 5 linear extinction lengths.

to that predicted by analytical consideration (see Fig. 4). For $y_r = -1.5$ the intensity dependence is close to the intensity dependence at the centre of the reflection region. For $y_r = 1.5$ the intensity due to nonlinearity shows a different behaviour.

The corresponding numerical calculations, performed for the reflection Si(220) [for which the reflection Si(440) is not forbidden] and for the same wavelength, do not depict any essential differences than is predicted by analytical consideration.

It should be mentioned that since the intensities are given in units of $I_{cr}/3$, *i.e.* are sufficiently less than the critical intensity, the perturbation nonlinear scattering theory on bound electrons is valid. Consequently, radiation and temperature damage may be ignored.

5. Conclusions

Bragg-case symmetrical two-wave third-order nonlinear dynamical diffraction of a monochromatic σ -polarized plane wave in a perfect crystal is considered theoretically. In the total reflection region for the special case of a forbidden $2h$ reflection an analytical solution in a semi-infinite non-absorbing crystal is found. Expressions for the total reflections' size and of the centre as a function of the intensity of the incidence wave are obtained. The centre of the total reflection region shifts to low incidence angles and the size of the total reflection region decreases with increasing intensity of the incidence wave. It was shown that in the nonlinear case the total reflection region exists for intensities below a certain maximal value. For the general case the results of numerical

calculations of nonlinear Takagi's equations in a semi-infinite absorbing perfect crystal are presented. The numerically obtained rocking curves behaviours confirm the predictions of the analytical consideration. A different behaviour of the opposite slopes (with respect to the centre) of the rocking curves is noticed. The same conclusion is true for intensity dependence on depth. The numerical calculations do not show any essential differences between forbidden $2h$ and not forbidden $2h$ reflections. The obtained behaviours of nonlinear diffraction are sufficiently sensitive to the intensity, which is given in units of $I_{cr}/3$. Consequently temperature and radiation damage may be ignored and the perturbation theory is valid.

Further developments of nonlinear dynamical diffraction can be investigation of the diffraction of spatially inhomogeneous beams (Gaussian beam *etc.*), nonlinear diffraction in deformed crystals (particularly bent crystals), asymmetric nonlinear diffraction and other nonlinear dynamical diffraction effects as well. The experiments can be performed using X-ray sources of synchrotron radiation and XFELs.

References

Authier, A. (2001). *Dynamical Theory of X-ray Diffraction*. Oxford University Press.

Balyan, M. K. (2015). *Crystallogr. Rep.* **60**. In the press.

Boyd, R. (2003). *Nonlinear Optics*. New York: Academic.

Conti, C., Fratolocchi, A., Ruocco, G. & Sette, F. (2008). *Opt. Express*, **16**, 8324–8331.

Doumy, G. *et al.* (2011). *Phys. Rev. Lett.* **106**, 083002.

Epelboin, Y. (1977). *Acta Cryst.* **A33**, 758–767.

James, R. W. (1950). *The Optical Principles of the Diffraction of X-rays*. London: G. Bell and Sons.

Nazarin, A., Podorov, S., Uschmann, I., Förster, E. & Sauerbrey, R. (2003). *Phys. Rev. A*, **67**, 041804.

Pinsker, Z. G. (1982). *X-ray Crystal Optics*. Moscow: Nauka. (In Russian.)

Prudnikov, A. P., Brychkov, Y. A. & Marichev, O. I. (1986). *Integrals and Series*, version 1. New York: Gordon and Breach.

Son, S.-K., Chapman, H. N. & Santra, R. (2011). *Phys. Rev. Lett.* **107**, 218102.

Takagi, S. (1969). *J. Phys. Soc. Jpn.* **26**, 1239–1253.

Tamasaku, K. & Ishikawa, T. (2007a). *Phys. Rev. Lett.* **98**, 244801.

Tamasaku, K. & Ishikawa, T. (2007b). *Acta Cryst.* **A63**, 437–438.

Tamasaku, K., Shigemasa, E., Inubushi, Y., Katayama, T., Sawada, K., Yumoto, H., Ohashi, H., Mimura, H., Yabashi, M., Yamauchi, K. & Ishikawa, T. (2014). *Nat. Photon.* **8**, 313–316.

Zambianchi, P. (2003). *Nonlinear Optics, Quantum Optics, and Ultrafast Phenomena with X-rays: Physics with X-rays Free Electron Lasers*, edited by B. W. Adams, pp. 287–326. New York: Springer Science + Business media.